Bimetallic Materials Based on Ag for Cathode/Anode Electrode in a Glucose Microfluidic Fuel Cell

F. M. Cuevas Muñiz[1], M. Guerra-Balcázar[1], J. Ledesma García[1], L. G. Arriaga[2,*]

[1]División de Investigación y Posgrado, Facultad de Ingeniería, Universidad Autónoma de Querétaro
Cerro de las Campanas S/N, Querétaro, Qro. C.P. 76010

[2]Centro de Investigación y Desarrollo Tecnológico en Electroquímica, Parque Tecnológico Querétaro Sanfandila S/N
Pedro Escobedo, Qro. C.P. 76703
email: larriaga@cideteq.mx

ABSTRACT

The present work shows the results for bimetallic materials PtAg/C and AuAg/C as cathode and anode electrode respectively in a microfluidic fuel cell with glucose as fuel in basic media. The electrodes were prepared for chemical reduction according to a modification of the Burst method and were characterized by XRD and electrochemical techniques. The fuel cell was able to harvest 600 mW cm^{-2}. The PtAg/C exhibits a better performance respect the commercial Pt/C at high concentrations of glucose. Meanwhile AuAg/C also contributed to stability of the fuel cell during long times of operation.

1. Introduction

Microfluidic fuel cells or membraneless fuel cells operate without a membrane as physical barrier to separate the anode and cathode. This membraneless laminar flow-based fuel cell (LFFC) design eliminates PEM-related issues of fuel crossover, anode dry-out, and cathode flooding. A fuel with greater interest because of their low cost is the Glucose [1–3]. The glucose fuel cells, utilizes noble metal catalysts such as platinum and gold [4]. Yet, the use of these metal catalysts has the great disadvantages that are easily poisoned due to fuel crossover. In this context the use of bimetallic catalysts is a viable solution because these materials shows belter electrocatalytic activities compared to the monometallic materials [5, 6]. With the further advantage that reduce the amount of inordinately expensive precious metals.

In this work, PtAg/C and AuAg/C bimetallic catalysts were synthesized and evaluated for the oxygen reduction reaction ORR and glucose oxidation reaction respectively in order to reduce the self-poisoning of the electrocatalysts on the microfluidic fuel cell. These catalyts were used in an microfluidic fuel cell and were comparated with Pt/C and Au/C catalyst.

2. Experimental

The bimetallic catalysts AuAg and PtAg were prepared following a previously reported procedure [5, 6]. For AuAg, a mix aqueous solution of $HAuCl_4$ (J.T. Baker) with $AgNO_3$ (J.T. Baker) was employed. Meanwhile for PtAg an aqueous solution of $H_2Pt(NO_2)_2SO_4$ (Alfa Aesar) with $AgNO_3$ (J.T. Baker) was used. In both cases, the aqueous solution was put together with tetraoctyl-ammonium bromide (Fluka) in toluene, and later Dodecanethiol (Aldrich) was added, and finally the metals were reduced with $NaBH_4$ (Aldrich). The nanoparticles were supported in vulcan carbon XC-72 (Cabot).

Physicochemical characterization was performed with TEM was accomplished using a JEOL JEM2200Fs + Cs STEM, and the X-ray diffraction was obtained using a Bruker D8 Advance diffractometer operated at 30 mV and 30 mA. The electrochemical tests were performed in a potentiostat BioLogic VSP. A conventional three electrode cell was employed. Hg,HgO electrode was used as reference electrode. A carbon bar was used as counter electrode. As working electrode an ink with the nanomaterials was employed and deposited in a glassy carbon disk electrode. The materials were tested in basic media (KOH 0.3 M) with oxygen saturated for PtAg/C or glucose 10 mM for AuAg/C.

The fuel cell was reported previously [7]. In the walls of the microchannel, the catalysts were placed by spray technique. Two streams of KOH 0.3 M, one containing oxygen saturated was placed in the cathodic side and other

with glucose 100 mM was placed in the anodic side. Later discharge curves were performed at 5 mV s^{-1} since OCP to 0 mV.

3. Results and discussion

3.1 Synthesis and characterization of AuAg/C and PtAg/C

The TEM micrographs are showed on figure 1. The AuAg/C micrograph is showed in the figure 1a. The results indicate the formation of nanoparticles of AuAg/C of composition 83-16 according the EDS results. The size of nanoparticles is around 16 nm. The figure 1b shows the TEM micrograph of PtAg/C. The TEM analysis showed that the particle structure had a core–shell type with a platinum center coated with silver. The EDS analysis of the catalyst revealed the mean composition of PtAg/C to be 81% Pt and 19% Ag. The composition in both catalysts are in close agreement with that of the metallic precursors that were used. The mean particle size of the PtAg nanoparticles is approximately 7 nm.

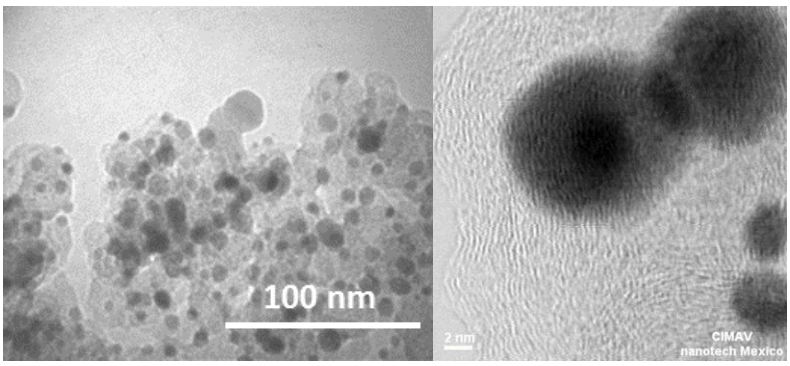

Figure 1. TEM micrograph of AuAg/C and PtAg/C catalysts.

The difractograms obtained were showed in figure 2. Crystalline planes of AuAg-based material are observed in Fig. 2a and located at 38.0°, 44.2°, 64.4°, 77.3° and 82°. The signals correspond to Au crystalline planes (1 1 1), (2 0 0), (2 2 0), (3 1 1) and (2 2 2). The value of lattice parameter is 4.089 Å and average particle size of 21 nm. The observed peaks are characteristic of a single face-centered-cubic (fcc) crystallographic structure of Au (JCPDS 04-0784). Variation of lattice parameter value suggests the presence of electronic interactions between outer electron shells of Ag and Au atoms, reducing the size of Ag atom [8]. This is an indicative of the formation of one phase in the material.

The figure 2b shows the X-ray diffraction pattern of PtAg/C, along with the characteristic peaks of a single fcc structure. The peaks located at 38°, 45°, 65°, 78° and 82° correspond to the same planes described above. The peak located at approximately 25° may be attributed to the graphite (0 0 2) crystalline plane of carbon. The lattice parameters calculated from this experimental data are 3.92 Å [9, 10]. The observed diffraction angles for the PtAg/C catalyst are located between those of the two pure metal elements Pt and Ag, suggesting the formation of alloy nanoparticles.

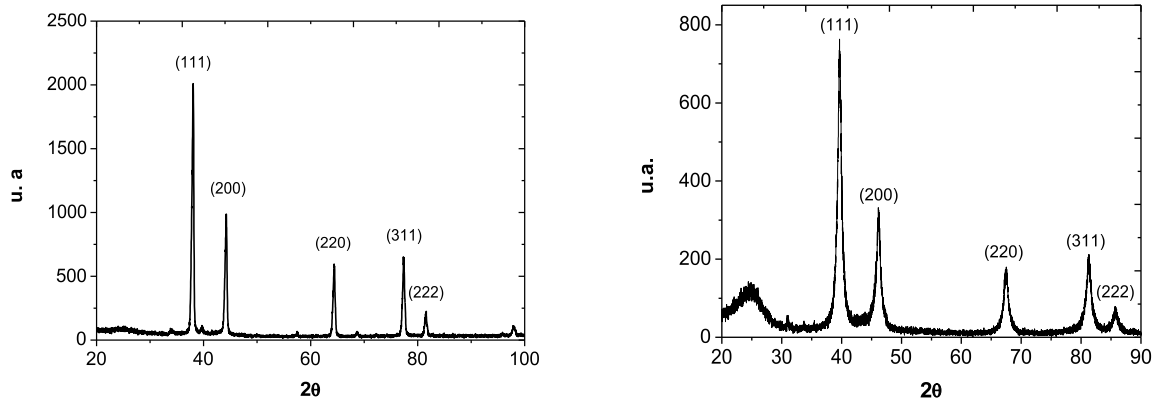

Figure 2. XRD patterns of (a) AuAg/C and (b) PtAg/C.

3.2 Electrochemical characterization

The voltametric profiles of (a) AuAg/C and (b) PtAg/C in basic media (KOH 0.3 M) and also Au/C, Ag/C y Pt/C for comparison are shown in the figure 3. For AuAg/C electrocatalyst are not observed the peaks corresponding to Ag oxides reduction, we can infer from this datum that that the bimetallic material are composed by a solid solution [11]. On the other hand the voltammetric profiles of PtAg/C, Pt/C and Ag/C electrodes in 0.3 M KOH under nitrogen atmosphere are compared. The Pt/C electrode shows the hydrogen adsorption and desorption to be located at 0.31 V vs. RHE. In the case of the Ag/C electrode, it is possible to observe an oxide peak around 1.1 V vs. RHE that corresponds to the formation of silver oxides. In the case of the PtAg/C catalyst, it sees a voltammetry similar to Pt/C, although both oxide and reduction peaks appear at 0.7 and 0.9 V vs. RHE, which is similar to the Ag/C catalyst [11].

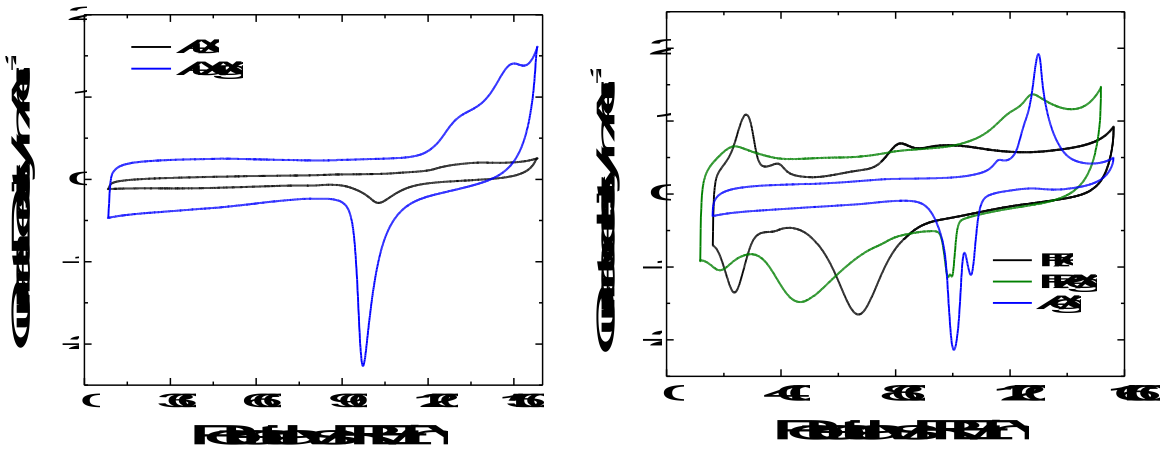

Figure 3. Voltammetric profile obtained in KOH 0.3 M at 20 mV s^{-1}

3.2.1 Glucose oxidation reaction

The response of AuAg/C for the glucose oxidation reaction was evaluated in presence of glucose 10 mM in basic media and compared to Au/C (figure 4). It is possible to observe a first signal in −225 and −380mV vs. RHE for Au/C and AuAg/C respectively, this process is related to the glucose oxidation to form gluconic acid [12, 13]. The AuAg/C electrocatalyst showed a negative shift ca. 150mV compared with Au/C for glucose electrooxidation. This observation point to that AuAg/C electrocatalyst favors the glucose electrooxidation as compared to Au/C. This behavior could be attributed to the interaction between bimetallic material and glucose. Yet, the mechanism of glucose oxidation involves adsorption of OH^- ions and this process is facilitated on Ag surfaces [14].

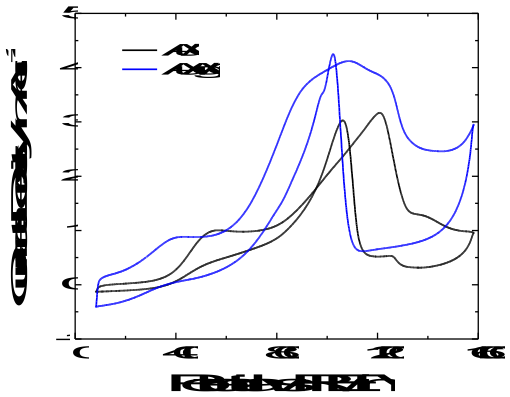

Figure 4. Cyclic voltammograms obtained on the Au/C and AuAg/C electrodes in 0.01M glucose + 0.3M KOH aqueous solution at 20mVs^{-1}.

3.2.2 Oxygen reduction reaction

To evaluate the catalytic activity of oxygen reduction reaction (ORR), polarization curves were obtained for the Ag/C, Pt/C and PtAg/C catalysts in 0.3 M KOH in an oxygen-saturated atmosphere using a rotatory disk electrode. The ORR curves for the PtAg/C, Pt/C and Ag/C catalysts are shown in Fig. 5 at 1600 rpm. The onset potential of the ORR is very similar for both Pt/C and PtAg/C (0.96 V vs. RHE), while the onset potential for Ag/C shows a negative shift of approximately 100 mV when compared with both Pt/C and PtAg/C. A higher current density is reached in the case of PtAg/C while using nearly 20% less loading than the Pt catalyst. These results show a better activity toward oxygen reduction reaction in an alkaline medium in the case of PtAg/C compared with Pt/C, which could be related to the synergistic relation between both metals as a bimetallic electrocatalyst.

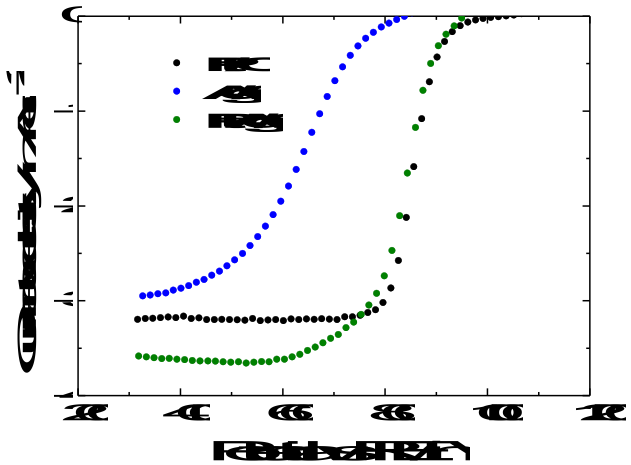

Figure 5. ORR polarization curves obtained in 0.3 M KOH under oxygen atmosphere.

3.4 Fuel cell tests

One fuel cell with PtAg/C (cathode) and AuAg/C (anode) was constructed and compared with a fuel cell with Pt/C (cathode) and Au/C (anode). The figure 6 show the performance of both cells with a solution of glucose 100 mM. The addition of silver allows a better performance at high concentrations of glucose. This result is attributed to tolerance to glucose for the cathode [6], and a better stability in the anodic side.

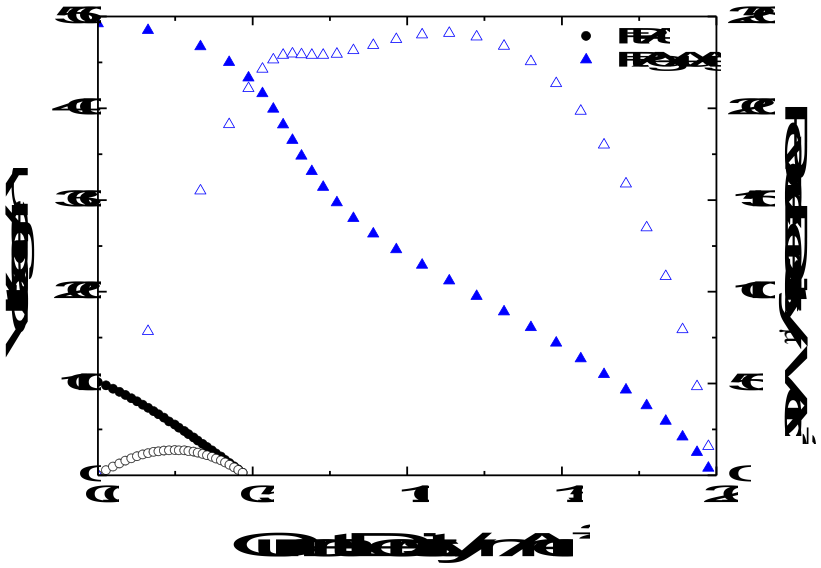

Figure 6. Discharge curves for monometallic and bimetallic microfluidic fuel cell.

4. Conclusions

The use of bimetallic alloy based in silver in catalysts for fuel cells can help the performance of this devices. In the case of glucose oxidation, the addition of silver reduce the potential of oxidation. For the oxygen reduction, the silver addition maintains the performance of the catalyst. Also the use of silver reduce the cost involved in the catalyst fabrication process.

5. Akcnowledgements

The authors to CONACYT for the economic support to this investigation.

6. References

[1]M. Guerra-Balcázar, D. Morales-Acosta, F. Castaneda, J. Ledesma-García, L.G. Arriaga, Electrochem. Commun. 12 (2010) 864.
[2] J. Ryu, H.-S. Kimb, H. Thomas, D. Lashmore, Biosens. Bioelectron. 25 (2010) 1603.
[3] C. Jin, I. Taniguchi, Mater. Lett. 61 (2007) 2365.
[4] A. Zebda, L. Renaud, M. Cretin, C. Innocent, F. Pichot, R. Ferrigno, S. Tingry, J. Power Sources 193 (2009) 602.
[5] F.M. Cuevas-Muñiz, M. Guerra-Balcázar, F. Castaneda, J. Ledesma-García, L.G. Arriaga, J. Power Sources 196 (2011) 5853.

[6] M. Guerra-Balcázar, F.M. Cuevas-Muñiz, L. Álvarez-Contreras, L.G. Arriaga, J. Ledesma-García, Journal of Power Sources 197 (2012) 121.

[7] M. Guerra-Balcázar, D. Morales-Acosta, F. Castaneda, J. Ledesma-García, L.G. Arriaga, Electrochem. Commun. 12 (2010) 864.

[8] N.N. Kariuki, J. Luo, M.M. Maye, S.A. Hassan, T. Menard, H.R. Naslund, Y. Lin, C. Wang, M.H. Engelhard, C.-J. Zhong, Langmuir 20 (2004) 11240.

[9] J.B. Xu, T.S. Zhao, Z.X. Liang, J. Phys. Chem. C 112 (2008) 17362.

[10] F.H.B. Lima, E.A. Ticianelli, Electrochim. Acta 49 (2004) 4091.

[11] M. Tominaga, T. Shimazoe, M. Nagashima, H. Kusuda, A. Kubo, Y. Kuwahara, I. Taniguchi, J. Electroanal. Chem. 590 (2006) 37.

[12] M. Tominaga, M. Nagashima, K. Nishiyama, I. Taniguchi, Electrochem. Commun. 9 (2007) 1892.

[13] M. Tominaga, M. Nagashima, K. Nishiyama, I. Taniguchi, Electrochem. Commun. 7 (2005) 189.

[14] V.A. Marichev, Electrochim. Acta 43 (1998) 2203.